



Rheological properties for inelastic Maxwell mixtures under shear flow

Vicente Garzó^{a,*}, Emmanuel Trizac^b

^a Departamento de Física, Universidad de Extremadura, E-06071 Badajoz, Spain

^b Laboratoire de Physique Théorique et Modèles Statistiques (CNRS UMR 8626), Bâtiment 100, Université Paris-Sud, 91405 Orsay cedex, France

ARTICLE INFO

Article history:

Received 17 November 2009

Received in revised form 11 January 2010

Accepted 13 January 2010

PACS:

05.20.Dd

45.70.Mg

51.10.+y

Keywords:

Uniform shear flow

Non-linear transport

Inelastic Maxwell models

Boltzmann equation

ABSTRACT

The Boltzmann equation for inelastic Maxwell models is considered to determine the rheological properties in a granular binary mixture in the simple shear flow state. The transport coefficients (shear viscosity and viscometric functions) are *exactly* evaluated in terms of the coefficients of restitution, the (reduced) shear rate and the parameters of the mixture (particle masses, diameters and concentration). The results show that in general, for a given value of the coefficients of restitution, the above transport properties decrease with increasing shear rate.

© 2010 Elsevier B.V. All rights reserved.

1. Introduction

It is well-recognized that granular matter can be modeled by a fluid of hard spheres with inelastic collisions. In the simplest version, the grains are assumed to be smooth so that the inelasticity is only accounted for by a constant coefficient of normal restitution. For sufficiently low-densities, the (inelastic) Boltzmann equation has been solved by means of the Chapman–Enskog method [1] and the Navier–Stokes transport coefficients have been obtained in terms of the coefficient of restitution [2]. Moreover, some analytical results in far from equilibrium situations have been also reported in the literature for inelastic hard spheres [3]. However, due to the complex mathematical structure of the Boltzmann collision operator, it is generally not possible to get exact results from the Boltzmann equation for inelastic hard spheres and consequently, most of the analytical results have been derived by using approximations and/or kinetic models.

As in the elastic case, a possible way to partially overcome the above difficulties is to consider the so-called inelastic Maxwell models (IMM), where the collision rate is independent of the rel-

ative velocity of the two colliding particles [4]. Thanks to this property, non-linear transport properties can be *exactly* obtained in some particular problems [5–7] for IMM without introducing additional and sometimes uncontrolled approximations. In addition, apart from their academic interest, it has also been shown that in some cases the results derived from IMM compare well with those obtained for inelastic hard spheres [5] and even recent experiments [8] for magnetic grains with dipolar interactions are well described by IMM. All these results stimulate the use of this interaction model as a toy model to characterize the influence of the inelasticity of collisions on the physical properties of granular fluids.

The aim of this paper is to determine the rheological properties (shear stress and normal stress differences) in a binary mixture described by the Boltzmann equation for IMM and subjected to the simple or uniform shear flow (USF). This state is perhaps one of the most widely studied states in granular gases [9]. At a macroscopic level, the USF is characterized by constant partial densities n_i , a uniform granular temperature T , and a linear velocity profile $u_x = ay$, where a is the constant shear rate. Under these conditions, the mass and heat fluxes vanish by symmetry and the pressure or stress tensor P_{ij} is the only relevant flux in the problem. Conservation of momentum implies $P_{i,y} = \text{const}$ while the energy balance equation reads

$$\frac{\partial}{\partial t} T = -\frac{2a}{dn} P_{xy} - T\zeta, \quad (1)$$

* Corresponding author.

E-mail addresses: vicenteg@unex.es (V. Garzó), trizac@lptms.u-psud.fr (E. Trizac).

URLs: <http://www.unex.es/eweb/fisteor/vicente/> (V. Garzó), <http://www.lptms.u-psud.fr/membres/trizac/> (E. Trizac).

where d is the dimensionality of the system ($d = 3$ for spheres and $d = 2$ for disks) and ζ is the inelastic cooling rate. Eq. (1) clearly shows that the temperature changes over time due to two competing effects: the viscous heating term aP_{xy} and the inelastic collisional cooling term ζT . While the first term is inherently positive (since $P_{xy} < 0$), the second term is negative since $\zeta > 0$. Depending on the initial condition, one of the effects prevails over the other one so that the temperature either decreases or increases in time, until a steady state is reached for sufficiently long times. Given that in this steady state the (reduced) shear rate is enslaved to the coefficients of restitution, the problem is inherently non-Newtonian (and so, beyond the scope of the Navier–Stokes description) in highly inelastic granular gases [10].

As in a previous paper for a single gas [7], the rheological properties of the granular gas are given in terms of a collision frequency ν_0 , which in principle can be freely chosen. Here we will consider two classes of IMM: (i) a collision frequency ν_0 independent of temperature (Model A) and (ii) a collision frequency $\nu_0(T)$ monotonically increasing with temperature (Model B). Model A is closer to the original model of Maxwell molecules for elastic gases [11,12] while Model B with $\nu_0(T) \propto \sqrt{T}$ is closer to inelastic hard spheres. The possibility of having a general temperature dependence of $\nu_0(T)$ for inelastic repulsive models has been recently introduced by Ernst and co-workers [13]. As will be shown later, Models A and B lead to the same results in the steady state limit. In particular, the reduced shear rate $a^* = a/\nu_0$ in the steady state is a *universal* function $a_s^*(\alpha_{ij})$ of the coefficients of restitution α_{ij} and the parameters of the mixture. However, since a^* does not change in time for Model A, a steady state does not exist except for the specific value $a^* = a_s^*(\alpha_{ij})$. Consequently, a non-Newtonian hydrodynamic regime (where a^* and α_{ij} are independent parameters) is reached in the long-time limit where the combined effect of both control parameters on the rheological properties can be studied analytically for Model A. This is an interesting new added value of this simple model.

The plan of the paper is as follows. We first introduce in Section 2 the Boltzmann equation framework for IMM; collisional moments are worked out. In Section 3 we will introduce driving through a macroscopic shear, and consider in particular the USF problem. We shall subsequently focus on rheological properties in Section 4, where our results for the non-linear shear viscosity and viscometric functions will be reported. Finally, conclusions will be drawn in Section 5.

2. The Boltzmann equation for IMM. Collisional moments

Let us consider a binary mixture of inelastic Maxwell gases at low density. In the absence of external forces, the set of non-linear Boltzmann equations for the mixture reads

$$\left(\frac{\partial}{\partial t} + \mathbf{v} \cdot \nabla\right) f_r(\mathbf{r}, \mathbf{v}; t) = \sum_s J_{rs}[\mathbf{v}|f_r(t), f_s(t)], \quad (2)$$

where $f_r(\mathbf{r}, \mathbf{v}_1; t)$ is the one-particle distribution function of species r ($r = 1, 2$) and the Boltzmann collision operator $J_{rs}[\mathbf{v}_1|f_r, f_s]$ describing the scattering of pairs of particles is

$$J_{rs}[\mathbf{v}_1|f_r, f_s] = \frac{\omega_{rs}}{n_s \Omega_d} \int d\mathbf{v}_2 \int d\hat{\sigma} [\alpha_{rs}^{-1} f_r(\mathbf{r}, \mathbf{v}_1, t) f_s(\mathbf{r}, \mathbf{v}_2, t) - f_r(\mathbf{r}, \mathbf{v}_1, t) f_s(\mathbf{r}, \mathbf{v}_2, t)]. \quad (3)$$

Here,

$$n_r = \int d\mathbf{v} f_r(\mathbf{v}) \quad (4)$$

is the number density of species r , ω_{rs} is an effective collision frequency (to be chosen later) for collisions of type $r - s$, $\Omega_d =$

$2\pi^{d/2}/\Gamma(d/2)$ is the total solid angle in d dimensions, and $\alpha_{rs} \leq 1$ refers to the constant coefficient of restitution for collisions between particles of species r with s . In addition, the primes on the velocities denote the initial values $\{\mathbf{v}'_1, \mathbf{v}'_2\}$ that lead to $\{\mathbf{v}_1, \mathbf{v}_2\}$ following a binary collision:

$$\mathbf{v}'_1 = \mathbf{v}_1 - \mu_{rs} (1 + \alpha_{rs}^{-1}) (\hat{\sigma} \cdot \mathbf{g}_{12}) \hat{\sigma}, \quad (5)$$

$$\mathbf{v}'_2 = \mathbf{v}_2 + \mu_{rs} (1 + \alpha_{rs}^{-1}) (\hat{\sigma} \cdot \mathbf{g}_{12}) \hat{\sigma}, \quad (6)$$

where $\mathbf{g}_{12} = \mathbf{v}_1 - \mathbf{v}_2$ is the relative velocity of the colliding pair, $\hat{\sigma}$ is a unit vector directed along the centers of the two colliding spheres, and $\mu_{rs} = m_r/(m_r + m_s)$.

The effective collision frequencies ω_{rs} are independent of velocity but depend on space and time through its dependence on density and temperature. Here, as in previous works [7] for monocomponent gases, we will assume that $\omega_{rs} \propto n_s T^q$, with $q \geq 0$. The case $q = 0$ (a collision frequency independent of temperature) will be referred to as Model A while the case $q > 0$ (collision frequency monotonically increasing with temperature) will be called Model B. Model A is closer to the original model of Maxwell molecules for elastic gases [11,12] while Model B, with $q = 1/2$, is closer to hard spheres.

Apart from n_r , at a hydrodynamic level, the relevant quantities in a binary mixture are the flow velocity \mathbf{u} , and the “granular” temperature T . They are defined in terms of moments of the distribution f_r as

$$\rho \mathbf{u} = \sum_r \rho_r \mathbf{u}_r = \sum_r \int d\mathbf{v} m_r \mathbf{v} f_r(\mathbf{v}), \quad (7)$$

$$nT = \sum_r n_r T_r = \sum_r \int d\mathbf{v} \frac{m_r}{d} V^2 f_r(\mathbf{v}), \quad (8)$$

where $\rho_r = m_r n_r$, $n = n_1 + n_2$ is the total number density, $\rho = \rho_1 + \rho_2$ is the total mass density, and $\mathbf{V} = \mathbf{v} - \mathbf{u}$ is the peculiar velocity. Eqs. (7) and (8) also define the flow velocity \mathbf{u}_r and the partial temperature T_r of species r , the latter measuring the mean kinetic energy of species r . As confirmed by computer simulations [14], experiments [15] and kinetic theory calculations [16], the global granular temperature T is in general different from the partial temperatures T_r .

The collision operators conserve the particle number of each species and the total momentum but the total energy is not conserved:

$$\int d\mathbf{v} J_{rs}[\mathbf{v}|f_r, f_s] = 0, \quad (9)$$

$$\sum_{r=1}^2 \sum_{s=1}^2 m_r \int d\mathbf{v} \mathbf{v} J_{rs}[\mathbf{v}|f_r, f_s] = 0, \quad (10)$$

$$\sum_{r=1}^2 \sum_{s=1}^2 m_r \int d\mathbf{v} V^2 J_{rs}[\mathbf{v}|f_r, f_s] = -dnT\zeta, \quad (11)$$

where ζ is identified as the total “cooling rate” due to inelastic collisions among all species. At a kinetic level, it is also convenient to discuss energy transfer in terms of the “cooling rates” ζ_r for the partial temperatures T_r . They are defined as

$$\zeta_r = \sum_s \zeta_{rs} = -\frac{1}{dn_r T_r} \sum_s \int d\mathbf{v} m_r V^2 J_{rs}[\mathbf{v}|f_r, f_s]. \quad (12)$$

The second equality in (12) defines ζ_{rs} . The total cooling rate ζ can be expressed in terms of the partial cooling rates ζ_r as

$$\zeta = T^{-1} \sum_{r=1}^2 x_r T_r \zeta_r, \quad (13)$$

where $x_r = n_r/n$ is the mole fraction of species r .

From Eqs. (9) to (11), the macroscopic balance equations for the mass, momentum and energy of the binary mixture can be easily obtained. They are given by

$$D_t n_r + n_r \nabla \cdot \mathbf{u} + \frac{\nabla \cdot \mathbf{j}_r}{m_r} = 0, \quad (14)$$

$$D_t \mathbf{u} + \rho^{-1} \nabla \cdot \mathbf{P} = \mathbf{0}, \quad (15)$$

$$D_t T - \frac{T}{n} \sum_{r=1}^2 \frac{\nabla \cdot \mathbf{j}_r}{m_r} + \frac{2}{dn} (\nabla \cdot \mathbf{q} + \mathbf{P} : \nabla \mathbf{u}) = -\zeta T. \quad (16)$$

In the above equations, $D_t = \partial_t + \mathbf{u} \cdot \nabla$ is the material derivative,

$$\mathbf{j}_r = m_r \int d\mathbf{v} \mathbf{V} f_r(\mathbf{v}), \quad (17)$$

is the mass flux for species r relative to the local flow,

$$\mathbf{P} = \sum_r \int d\mathbf{v} m_r \mathbf{V} \mathbf{V} f_r(\mathbf{v}), \quad (18)$$

is the total pressure tensor, and

$$\mathbf{q} = \sum_r \int d\mathbf{v} \frac{1}{2} m_r V^2 \mathbf{V} f_r(\mathbf{v}) \quad (19)$$

is the total heat flux.

The main advantage of the Boltzmann equation for Maxwell models (both elastic and inelastic) is that the (collisional) moments of $J_{rs}[f_r, f_s]$ can be exactly evaluated in terms of the moments of f_r and f_s without the explicit knowledge of both distribution functions [11]. This property has been recently exploited [20] to obtain the detailed expressions for all the second-, third- and fourth-degree collisional moments for a monodisperse gas. In the case of a binary mixture, only the first- and second-degree collisional moments have been also explicitly obtained. In particular [5],

$$\begin{aligned} \int d\mathbf{v} m_r \mathbf{V} \mathbf{V} J_{rs}[f_r, f_s] &= -\frac{\omega_{rs}}{\rho_s d} \mu_{sr} (1 + \alpha_{rs}) \left\{ 2\rho_s \mathbf{P}_r - (\mathbf{j}_r \cdot \mathbf{j}_s + \mathbf{j}_s \cdot \mathbf{j}_r) \right. \\ &\quad - \frac{2}{d+2} \mu_{sr} (1 + \alpha_{rs}) [\rho_s \mathbf{P}_r + \rho_r \mathbf{P}_s - (\mathbf{j}_r \cdot \mathbf{j}_s + \mathbf{j}_s \cdot \mathbf{j}_r) \\ &\quad \left. + \left[\frac{d}{2} (\rho_r p_s + \rho_s p_r) - \mathbf{j}_r \cdot \mathbf{j}_s \right] \mathbb{1} \right\}, \end{aligned} \quad (20)$$

where

$$\mathbf{P}_r = \int d\mathbf{v} m_r \mathbf{V} \mathbf{V} f_r, \quad (21)$$

$p_r = n_r T_r = \text{tr} \mathbf{P}_r / d$ is the partial pressure of species r , and $\mathbb{1}$ is the $d \times d$ unit tensor. It must be remarked that, in general beyond the linear hydrodynamic regime (Navier–Stokes order), the above property of the Boltzmann collision operator is not sufficient to exactly solve the hierarchy of moment equations due to the free-streaming term of the Boltzmann equation. Nevertheless, there exist some particular situations (such as the simple shear flow problem) for which the above hierarchy can be recursively solved.

The cooling rates ζ_{rs} defined by Eq. (12) can be easily obtained from Eq. (20) as

$$\zeta_{rs} = \frac{2\omega_{rs}}{d} \mu_{sr} (1 + \alpha_{rs}) \left[1 - \frac{\mu_{sr}}{2} (1 + \alpha_{rs}) \frac{\theta_r + \theta_s}{\theta_s} + \frac{\mu_{sr} (1 + \alpha_{rs}) - 1}{d \rho_s p_r} \mathbf{j}_r \cdot \mathbf{j}_s \right], \quad (22)$$

where

$$\theta_r = \frac{m_r}{\gamma_r} \sum_s m_s^{-1}, \quad (23)$$

and $\gamma_r \equiv T_r/T$. Eq. (22) provides the relationship between the collision frequencies ω_{rs} and the cooling rates ζ_{rs} . This relationship can be used to fix the explicit forms of ω_{rs} . As in previous works on inelastic Maxwell mixtures [5,21], ω_{rs} is chosen here to guarantee that the cooling rate for IMM be the same as that of inelastic hard spheres (evaluated at the local equilibrium approximation) [16]. With this choice, one gets

$$\omega_{rs} = x_s \left(\frac{\sigma_{rs}}{\sigma_{12}} \right)^{d-1} \left(\frac{\theta_r + \theta_s}{\theta_r \theta_s} \right)^{1/2} v_0, \quad v_0 = A(q) n T^q, \quad (24)$$

where the value of the quantity $A(q)$ is irrelevant for our purposes. Upon deriving (24) use has been made of the fact that the mass flux \mathbf{j}_r vanishes in the local equilibrium approximation. In the remainder of this paper, we will take the choice (24) for ω_{rs} . The results for IMM [5] obtained with the latter choice in the *steady* shear flow problem compare very well with those theoretically obtained for inelastic hard spheres in the first Sonine approximation and by means of Monte Carlo simulations [22].

3. Uniform shear flow

Let us assume that the binary mixture is under USF. The USF state is macroscopically defined by constant densities n_r , a spatially uniform temperature $T(t)$ and a linear velocity profile $\mathbf{u}(y) = \mathbf{u}_1(y) = a y \hat{\mathbf{x}}$, where a is the *constant* shear rate. Since n_r and T are uniform, then $\mathbf{j}_r = \mathbf{q} = \mathbf{0}$, and the transport of momentum (measured by the pressure tensor) is the relevant phenomenon. At a microscopic level, the USF is characterized by a velocity distribution function that becomes *uniform* in the local Lagrangian frame, i.e., $f_r(\mathbf{r}, \mathbf{v}; t) = f_r(\mathbf{V}, t)$. In this frame, the Boltzmann equation (2) reads [12]

$$\frac{\partial}{\partial t} f_1 - a V_y \frac{\partial}{\partial V_x} f_1 = J_{11}[f_1, f_1] + J_{12}[f_1, f_2] \quad (25)$$

and a similar equation for f_2 . Eq. (25) is invariant under the transformations $(V_x, V_y) \rightarrow (-V_x, -V_y)$, $V_i \rightarrow -V_i$, with $i \neq x, y$. This implies that if the initial state is compatible with the latter symmetry properties, then the solution to (25) has the same properties at any time $t > 0$. Note that the properties of uniform temperature and constant densities and shear rate are enforced in computer simulations by applying the Lees–Edwards boundary conditions [17], regardless of the particular interaction model considered. In the case of boundary conditions representing realistic plates in relative motion, the corresponding non-equilibrium state is the so-called Couette flow, where densities, temperature and shear rate are no longer uniform [18,19].

As said before, the rheological properties of the mixture are obtained from the pressure tensor $\mathbf{P} = \mathbf{P}_1 + \mathbf{P}_2$, where the partial pressure tensors \mathbf{P}_r ($r = 1, 2$) are defined by Eq. (21). The elements of these tensors can be obtained by multiplying the Boltzmann equation (25) by $m_r \mathbf{V} \mathbf{V}$ and integrating over \mathbf{V} . The result is

$$\frac{\partial}{\partial t} P_{1,ij} + a_{ik} P_{1,kj} + a_{jk} P_{1,ki} + B_{11} P_{1,ij} + B_{12} P_{2,ij} = (A_{11} p_1 + A_{12} p_2) \delta_{ij}, \quad (26)$$

where use has been made of Eq. (20) (with $\mathbf{j}_r = \mathbf{0}$). In Eq. (26), $a_{ij} = a \delta_{ix} \delta_{jy}$ and we have introduced the coefficients

$$A_{11} = \frac{\omega_{11}}{2(d+2)} (1 + \alpha_{11})^2 + \frac{\omega_{12}}{d+2} \mu_{21}^2 (1 + \alpha_{12})^2, \quad (27)$$

$$A_{12} = \frac{\omega_{12}}{d+2} \frac{\rho_1}{\rho_2} \mu_{21}^2 (1 + \alpha_{12})^2, \quad (28)$$

$$B_{11} = \frac{\omega_{11}}{d(d+2)}(1 + \alpha_{11})(d + 1 - \alpha_{11}) + \frac{2\omega_{12}}{d(d+2)}\mu_{21}(1 + \alpha_{12})[d + 2 - \mu_{21}(1 + \alpha_{12})], \quad (29)$$

$$B_{12} = -\frac{2}{d}A_{12}. \quad (30)$$

A similar equation can be obtained for P_2 , by adequate change of indices $1 \leftrightarrow 2$. The balance equation (1) for the temperature can be easily obtained from Eq. (26). In reduced units, Eq. (1) can be written as

$$\nu_0^{-1} \frac{\partial}{\partial t} \ln T = -\zeta^* - \frac{2a^*}{d} P_{xy}^*, \quad (31)$$

where $\zeta^* = \zeta/\nu_0$, $a^* = a/\nu_0$, $P_{xy}^* = P_{xy}/p$, $p = nT$ being the hydrostatic pressure. The expression for ζ^* can be obtained from Eqs. (12), (13) and (22) when one takes $\mathbf{j}_r = \mathbf{0}$. It is given by

$$\zeta^* = \frac{2}{d} \sum_{r=1}^2 \sum_{s=1}^2 x_r x_s \left(\frac{\sigma_{rs}}{\sigma_{12}} \right)^{d-1} \left(\frac{\theta_r + \theta_s}{\theta_r \theta_s} \right)^{1/2} \gamma_r \mu_{sr} (1 + \alpha_{sr}) \times \left[1 - \frac{\mu_{sr}}{2} (1 + \alpha_{rs}) \frac{\theta_r + \theta_s}{\theta_s} \right]. \quad (32)$$

As said in Section 1, Eq. (31) shows that the temperature changes in time due the competition of two opposite mechanisms: on the one hand, viscous heating (shearing work) and, on the other hand, energy dissipation in collisions. Moreover, the reduced shear rate a^* is the non-equilibrium relevant parameter of the USF problem since it measures the distance of the system from the homogeneous cooling state. It is apparent that, except for Model A ($q = 0$), the collision frequency $\nu_0(T) \propto T^q$ is an increasing function of temperature (provided $q > 0$), and so $a^*(t) \propto T(t)^{-q}$ is a function of time. Consequently, for $q \neq 0$, after a transient regime a steady state is achieved in the long time limit when both viscous heating and collisional cooling cancel each other and the mixture autonomously seeks the temperature at which the above balance occurs. In this steady state, the reduced shear rate and the coefficients of restitution are not independent parameters since they are related through the steady state condition

$$a_s^* P_{s,xy}^* = -\frac{d}{2} \zeta^*, \quad (33)$$

where we have called a_s^* and $P_{s,xy}^*$ the steady-state values of the (reduced) shear rate and the pressure tensor. On the other hand, when $q = 0$, $\partial_t a^* = 0$ and the reduced shear rate remains in its initial value regardless of the values of the coefficients of restitution α_{rs} . As a consequence, in the case of Model A, there is no steady state (unless a^* takes the specific value a_s^* given by the condition (33)) and a^* and α_{rs} are independent parameters in the USF problem. The analytical study of the combined effect of both control parameters on the pressure tensor is the main goal of this paper.

4. Rheological properties

In order to characterize the non-linear response of the system to the action of strong shearing, it is convenient to introduce the (reduced) non-linear shear viscosity η^* and the (reduced) viscometric functions Ψ_1^* and Ψ_2^* as

$$\eta^*(a^*) = -\frac{\nu_0}{p} \frac{P_{xy}}{a}, \quad (34)$$

$$\Psi_1^*(a^*) = \frac{\nu_0^2}{p} \frac{P_{xx} - P_{yy}}{a^2}, \quad \Psi_2^*(a^*) = \frac{\nu_0^2}{p} \frac{P_{zz} - P_{yy}}{a^2}. \quad (35)$$

The viscosity function $\eta^*(a^*)$ is a measure of the breakdown of the linear relationship between the shear stress P_{xy} and the shear rate (Newton's law), while the first and second viscometric functions $\Psi_{1,2}^*(a^*)$ represent the normal stress differences. The explicit form of the above functions depends on the interaction model considered.

4.1. Model A

In Model A ($q = 0$), the collision frequency is independent of temperature and the reduced shear rate a^* is a constant. Thus, Eq. (26) and its counterpart for P_2 constitute a linear homogeneous set of coupled differential equations. In fact, it is easy to see that the relevant elements of the partial pressure tensors are the xy -elements along with the diagonal ones. As expected, the remaining elements tend to zero in the long-time limit. Moreover, from Eq. (26) is also easy to prove that, for long times, $P_{r,yy} = P_{r,zz} = \dots = P_{r,dd}$. Thus, according to Eq. (35), the second viscometric function $\Psi_2^* = 0$. This is a particular property of IMM since $\Psi_2^* \neq 0$ for inelastic hard spheres [22], although its magnitude is always much smaller than that of Ψ_1^* . As a consequence, the relevant elements of the partial pressure tensors are $P_{r,xx} = p_r - (d - 1)P_{r,yy}$, $P_{r,yy}$, and $P_{r,xy}$ with $r = 1, 2$.

As in the monocomponent granular case [7], one can check that, after a certain kinetic regime lasting a few collision times, the scaled pressure tensors $P_{r,ij}^* = P_{r,ij}/p$ reach well-defined stationary values (non-Newtonian hydrodynamic regime), which are non-linear functions of the (reduced) shear rate $a^* = a/\nu_0$ and the coefficients of restitution. In terms of these scaled variables and by using matrix notation, Eq. (26) can be rewritten as

$$\mathcal{L}\mathcal{P} = \mathcal{Q}, \quad (36)$$

where \mathcal{P} is the column matrix defined by the set

$$\mathcal{P} \equiv \{P_{1,xx}^*, P_{1,yy}^*, P_{1,xy}^*, P_{2,xx}^*, P_{2,yy}^*, P_{2,xy}^*\}, \quad (37)$$

\mathcal{Q} is the column matrix

$$\mathcal{Q} = \begin{pmatrix} A_{11}^* p_1^* + A_{12}^* p_2^* \\ A_{11}^* p_1^* + A_{12}^* p_2^* \\ 0 \\ A_{22}^* p_2^* + A_{21}^* p_1^* \\ A_{22}^* p_2^* + A_{21}^* p_1^* \\ 0 \end{pmatrix}, \quad (38)$$

and \mathcal{L} is the square matrix

$$\mathcal{L} = \begin{pmatrix} B_{11}^* + \lambda & 0 & 2a^* & B_{12}^* & 0 & 0 \\ 0 & B_{11}^* + \lambda & 0 & 0 & B_{12}^* & 0 \\ 0 & a^* & B_{11}^* + \lambda & 0 & 0 & B_{12}^* \\ B_{21}^* & 0 & 0 & B_{22}^* + \lambda & 0 & 2a^* \\ 0 & B_{21}^* & 0 & 0 & B_{22}^* + \lambda & 0 \\ 0 & 0 & B_{21}^* & 0 & a^* & B_{22}^* + \lambda \end{pmatrix}. \quad (39)$$

Here, $p_r^* = p_r/p = x_r \gamma_r$, $A_{rs}^* = A_{rs}/\nu_0$ and $B_{rs}^* = B_{rs}/\nu_0$. Moreover, on physical grounds it has been assumed that for long times the temperature behaves as

$$T(t) = T(0)e^{\lambda \nu_0 t}, \quad (40)$$

where λ is also a non-linear function of a^* , α_{rs} and the parameters of the mixture. The (reduced) total pressure tensor $P_{ij}^* = P_{ij}/p$ of the

mixture is defined as

$$P_{ij}^* = P_{1,ij}^* + P_{2,ij}^* \tag{41}$$

The solution to Eq. (36) is

$$\mathcal{P} = \mathcal{L}^{-1} \cdot \mathcal{Q}. \tag{42}$$

The explicit forms for $P_{1,xx}^*$, $P_{1,yy}^*$, and $P_{1,xy}^*$ can be found in the Appendix A. The corresponding expressions for species 2 are easily obtained by adequately changing the indices. This solution is still formal as we do not know the shear-rate dependence of λ and the temperature ratios γ_1 and γ_2 . These quantities must be consistently determined from the requirements

$$x_1 \gamma_1 = \frac{P_{1,xx}^* + (d-1)P_{1,yy}^*}{d}, \tag{43}$$

$$x_2 \gamma_2 = \frac{P_{2,xx}^* + (d-1)P_{2,yy}^*}{d}, \tag{44}$$

$$\gamma_2 = \frac{1 - x_1 \gamma_1}{x_2}, \tag{45}$$

which follows from Eq. (8). Since the collision frequencies ω_{rs} are non-linear functions of the temperature ratios, then it is not possible to get a closed equation for λ or γ_r . Thus, one has to numerically solve the set of non-linear equations (43) and (44).

Nevertheless, there are some limiting cases for which the problem can be solved analytically. For instance, in the case of mechanically equivalent particles ($m_1 = m_2, \sigma_1 = \sigma_2, \alpha_{11} = \alpha_{22} = \alpha_{12} \equiv \alpha$), one gets that $\gamma_1 = \gamma_2 = 1$ and the partial pressure tensors $P_{r,ij}^*$ can be written as

$$\frac{P_{1,yy}^*}{x_1} = \frac{P_{2,yy}^*}{x_2} = \frac{1}{1 + 2\Lambda}, \tag{46}$$

$$\frac{P_{1,xx}^*}{x_1} = \frac{P_{2,xx}^*}{x_2} = \frac{1 + 2d\Lambda}{1 + 2\Lambda}, \tag{47}$$

$$\frac{P_{1,xy}^*}{x_1} = \frac{P_{2,xy}^*}{x_2} = -\frac{\tilde{a}}{(1 + 2\Lambda)^2}, \tag{48}$$

where

$$\tilde{a} = \frac{2(d+2)}{(1+\alpha)^2} a^*, \tag{49}$$

and Λ is the real root of the equation

$$\Lambda(1 + 2\Lambda)^2 = \frac{\tilde{a}^2}{d}, \tag{50}$$

namely,

$$\Lambda(\tilde{a}) = \frac{2}{3} \sinh^2 \left[\frac{1}{6} \cosh^{-1} \left(1 + \frac{27}{d} \tilde{a}^2 \right) \right]. \tag{51}$$

The parameter λ governing the long-time behaviour of the temperature can be easily obtained from Eqs. (31) and (40) as

$$\lambda = -\zeta^* - \frac{2a^*}{d} P_{xy}^* = \frac{(1+\alpha)^2}{d+2} \Lambda - \frac{1-\alpha^2}{2d} \tag{52}$$

where use has been made of the result $\zeta^* = (1-\alpha^2)/2d$. Eqs. (46)–(52) are the same as those obtained for a monocomponent gas [7,24]. Moreover, in the absence of shear field ($a^* = 0$), $P_{r,xx}^* = P_{r,yy}^* = x_r \gamma_r$ and the shear viscosity function $\eta^* = \eta_1^* + \eta_2^*$ where

$$\eta_1^* = \frac{x_1 \gamma_1 (B_{22}^* - \zeta^*) + x_2 \gamma_2 B_{12}^*}{(B_{11}^* - \zeta^*)(B_{22}^* - \zeta^*) - B_{12}^* B_{21}^*}, \quad 1 \leftrightarrow 2. \tag{53}$$

The temperature ratio $\gamma = \gamma_1/\gamma_2$ is determined from the condition

$$\frac{x_1}{x_2} \gamma = \frac{P_{1,xx}^* + (d-1)P_{1,yy}^*}{P_{2,xx}^* + (d-1)P_{2,yy}^*}. \tag{54}$$

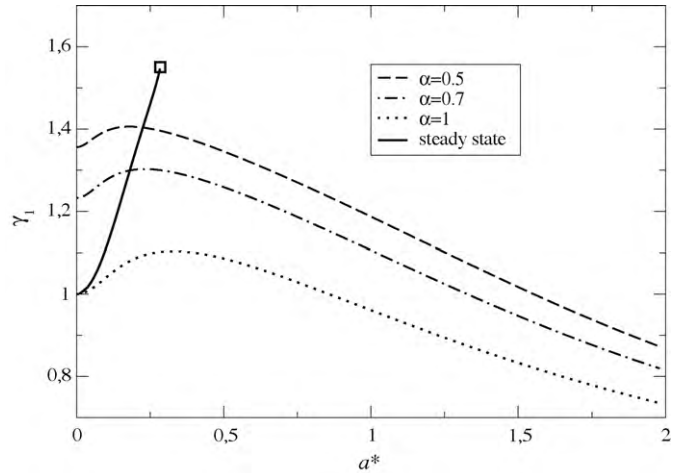


Fig. 1. Shear rate dependence of the temperature ratio $\gamma_1 = T_1/T$ in three dimensions ($d = 3$), for an equimolar mixture ($x_1 = 0.5$), with $\sigma_1/\sigma_2 = 2$, and $m_1/m_2 = 8$. Three values of the common coefficient of restitution ($\alpha \equiv \alpha_{11} = \alpha_{12} = \alpha_{22}$) are displayed, together with the stationary curve, also shown in Fig. 7 (see text for details). The continuous thick curve shows the locus of steady-state results (also shown in Fig. 7) when dissipation is scanned in the admissible range $\alpha \in [0, 1]$. The square locates the terminal shear rate at maximum dissipation.

These results are consistent with those obtained for IMM in the Navier–Stokes regime [21].

It must be remarked that, although the scaled pressure tensors $P_{r,ij}^*$ reach stationary values, the gas is not in general in a steady state since the temperature changes in time. Actually, according to Eqs. (31) and (34), one gets

$$v_0^{-1} \partial_t \ln T = -\zeta^* + \frac{2a^{*2}}{d} \eta^*. \tag{55}$$

Eq. (55) shows that $T(t)$ either grows or decay exponentially. The first situation occurs if $2a^{*2}\eta^* > d\zeta^*$. In that case, the imposed shear rate is sufficiently large (or the inelasticity is sufficiently low) as to make the viscous heating effect dominate over the inelastic cooling. The opposite happens if $d\zeta^* > 2a^{*2}\eta^*$. A perfect balance between both effects takes place when $2a^{*2}\eta^* = d\zeta^*$.

The expressions for the rheological functions $\eta^*(a^*)$ and $\Psi_1^*(a^*)$ depend on many parameters: $\{x_1, m_1/m_2, \sigma_1/\sigma_2, \alpha_{11}, \alpha_{22}, \alpha_{12}, a^*\}$. Obviously, this complexity exists in the elastic case as well [23], so that the primary new feature is the dependence of $\eta^*(a^*)$ and $\Psi_1^*(a^*)$ on dissipation, on which we shall concentrate. Also, for simplicity, we take the simplest case of common coefficient of restitution ($\alpha_{11} = \alpha_{22} = \alpha_{12} \equiv \alpha$). This reduces the parameter space to five quantities: $\{x_1, m_1/m_2, \sigma_1/\sigma_2, \alpha, a^*\}$. Before considering the rheological functions $\eta^*(a^*)$ and $\Psi_1^*(a^*)$, it is interesting to analyze the dependence of the temperature ratio T_1/T_2 on the shear rate. This quantity measures the lack of equipartition of the kinetic energy. Obviously, $T_1 = T_2$ for any value of the shear rate and/or the coefficient of restitution in the case of mechanically equivalent particles. Fig. 1 shows the temperature ratio as a function of shear rate in a situation where the grains have the same mass density [$(\sigma_1/\sigma_2)^d = m_1/m_2$]. As is often the case in driven binary granular gases, the more massive particles have a larger granular temperature for moderate shear rates, while the reverse conclusion holds at high shears. The inelasticity parameter α and shear rate a^* are here considered as independent, which in general results in an unsteady situation for the system. The intersection of a curve $\gamma_1(a^*)$ for a given α with the steady state line shown by the continuous thick line, provides the shear rate a_s^* corresponding to an exact balance between viscous heating and inelastic dissipation. For $a^* > a_s^*$, the temperature diverges, while it decays to 0 in the opposite case.

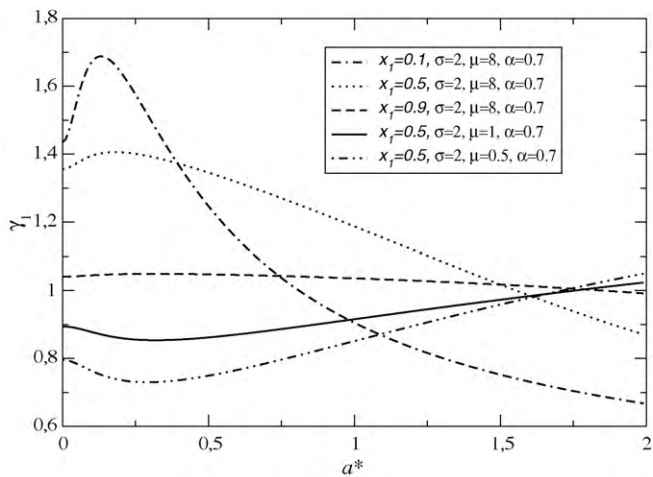


Fig. 2. Temperature ratio $\gamma_1 = T_1/T$ as a function of the reduced shear rate a^* in three dimensions ($d = 3$). Here, $\sigma \equiv \sigma_1/\sigma_2$ denotes the size ratio while $\mu \equiv m_1/m_2$ is the mass ratio.

We note that even in the elastic case, the temperature ratio differs from unity, as a signature of non-equilibrium behaviour. Only when the shear rate does vanish do we recover the equilibrium equipartition result ($\gamma_1 = 1$). Fixing dissipation at $\alpha = 0.7$, Fig. 2 complements the results of Fig. 1 by showing the influence of mixture composition x_1 . The same qualitative trends are observed as in Fig. 1, see the three upper curves. However, Fig. 2 also shows that changing the mass ratio (other parameters being fixed) can alter the results and lead to an increasing ratio T_1/T with increasing a^* .

It appears that the non-linear viscosity and viscometric function exhibit a more robust behaviour with shear rate. It can be seen in Fig. 3 that those functions decrease with increasing a^* . In this figure, the steady state values are shown with the continuous thick curve, and the maximum possible stationary shear rate is indicated by the squares (which correspond to $\alpha = 0$). As above, for a given inelasticity, the intersection of the η^* (resp Ψ_1^*) curve with its steady-state counterpart determines the steady-state value of the shear-rate (resp normal stress difference). As in Fig. 1, three coefficients of restitution have been chosen in Fig. 3, and correspond

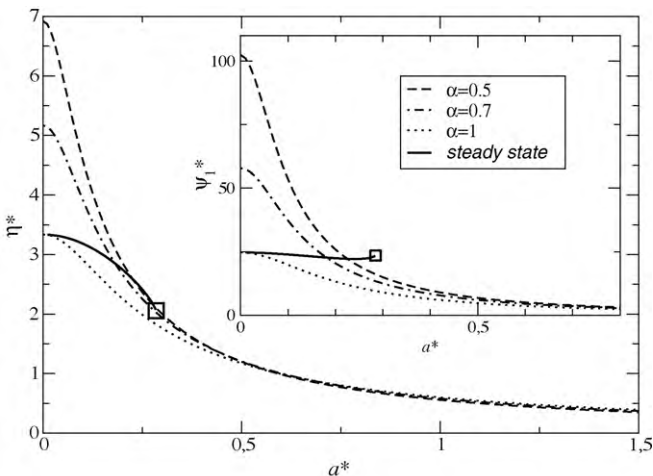


Fig. 3. Shear rate dependence of the reduced non-linear shear viscosity η^* for $d = 3$, an equimolar mixture ($x_1 = 0.5$), $\sigma_1/\sigma_2 = 2$, and $m_1/m_2 = 8$, for three values of the (common) coefficient of restitution α (same situation as in Fig. 1). The inset shows Ψ_1^* versus the reduced shear rate a^* . The continuous thick curves are the loci of steady-state results (also shown in Fig. 7) when dissipation is scanned in the admissible range $\alpha \in [0, 1]$. The squares locate the terminal shear rate at maximum dissipation.

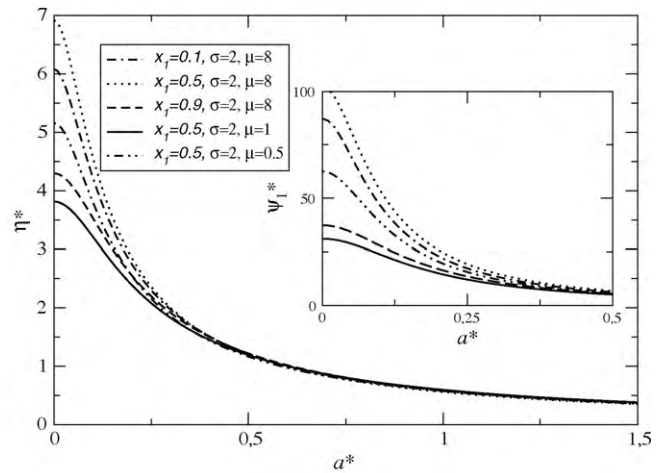


Fig. 4. Non-linear shear viscosity η^* and normal stress difference Ψ_1^* versus a^* . The parameters are the same as for Fig. 2, and the different curve styles have the same meaning as in Fig. 2.

to strongly inelastic ($\alpha = 0.5$), moderately inelastic ($\alpha = 0.7$), and elastic systems ($\alpha = 1$). For completeness, we also show in Fig. 4 the rheological functions corresponding to the parameter set of Fig. 2. The same qualitative trend is observed as in Fig. 3. We note in Figs. 3 and 4 the systematic trend that at high shear rates, the viscosity and normal stress difference become practically insensitive to the parameters specifying the state of the system, in particular dissipation, although the different curves do not converge onto a single master curve when $a^* \rightarrow \infty$. This observation is reminiscent of the single species phenomenology [7]. We also observe that the dependence on mixture composition x_1 and mass ratio is more subtle (see e.g. the $\sigma_1/\sigma_2 = 2$ and $m_1/m_2 = 8$ curves showing that the largest shear stress and normal stress difference occur in the equimolar case). Likewise, it is observed that for $x_1 = 0.5, \sigma_1/\sigma_2 = 2$, the smallest shear stress and normal stress difference correspond to like masses ($m_1 = m_2$). We do not dwell on those effects since they are already present in the vanishing shear rate limit. A non-trivial effect of shear rate, however, is illustrated in Fig. 5: whereas at small a^* , the viscosity function decreases with increasing α (at least in the physically relevant range $\alpha > 0.7$), increasing the shear rate leads to the opposite effect (see the inset of Fig. 5). Enhanced dissipation then leads to smaller shear stresses. In Fig. 5, we have displayed the full possible range $0 \leq \alpha \leq 1$ to show that even at small shear

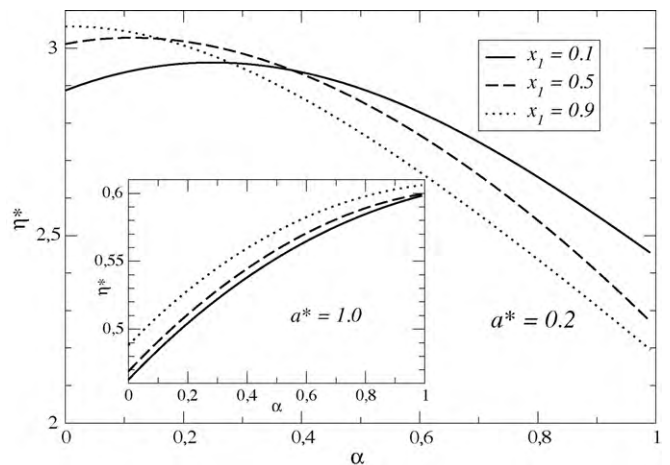


Fig. 5. Non-linear shear viscosity η^* for $d = 3, \sigma_1/\sigma_2 = 2$, and $m_1/m_2 = 8$, as a function of the (common) coefficient of restitution α , for three mole fractions x_1 . The main graph is for $a^* = 0.2$ and the inset is for $a^* = 1$.

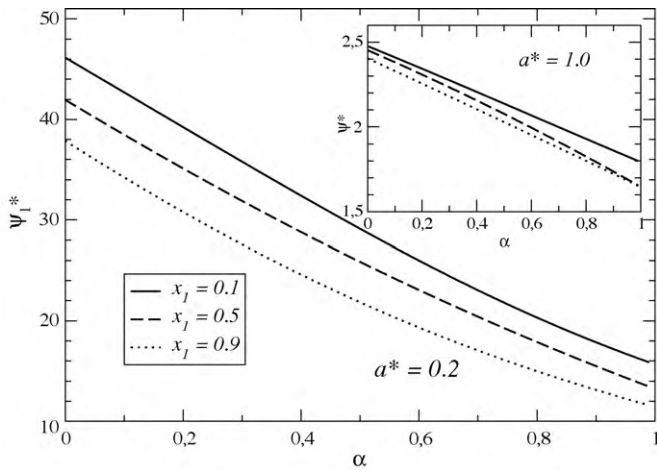


Fig. 6. Same as Fig. 5, but for the normal stress difference Ψ_1^* .

rates, an extreme dissipation can lead to a decreasing viscosity. We finally note here that those effects are absent for the normal stress difference, that appears to be a decreasing function of α , see Fig. 6.

4.2. Model B

In Model B the collision frequency $\nu_0(T)$ is an increasing function of temperature, and so the reduced shear rate a^* is not constant. In order to have $\eta^*(a^*)$ and $\Psi_1^*(a^*)$ in Model B, one has to solve numerically the non-linear set (26), discard the kinetic stage of the evolution, and eliminate time in favor of $a^*(t)$ [7,10]. In addition, it should be remembered that the above functions depend on the temperature ratio, that is itself time dependent through its dependence on $a^*(t)$. The above task in the case of a mixture is therefore a significantly more complex problem than in the monodisperse case. However, the results derived in the single gas case [7] indicate that the influence of the temperature dependence of ν_0 on the rheological properties is quite small. We then restrict here our discussion to the steady-state solution for Model B. In this case, it is easy to see that the results obtained in the steady simple shear flow state are *universal* in the sense that they apply both for Model A and Model B, regardless of the specific dependence of ν_0 on T .

Fig. 7 shows the corresponding rheological functions and temperature ratio obtained at long times for a selected parameter set. The figure also illustrates that in the steady state, dissipation and reduced shear are coupled (see the graph on the right hand side):

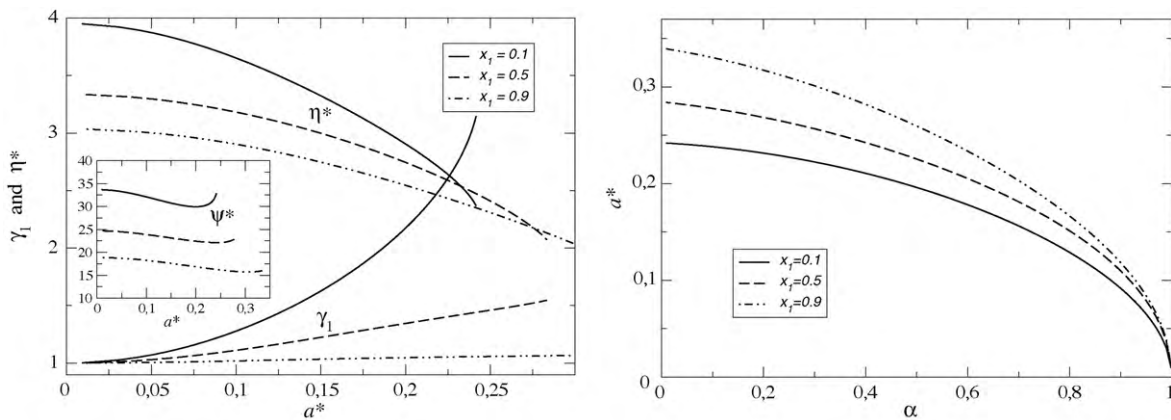


Fig. 7. (left) Plots of the temperature ratio $\gamma_1 = T_1/T$ and the non-linear shear viscosity η^* as functions of the (reduced) shear rate a^* in the steady state for $d = 3$, $\sigma_1/\sigma_2 = 2$, $m_1/m_2 = 8$, that corresponds to grains of same mass density. Three different compositions x_1 are displayed. The inset shows the normal stress difference $\psi^* \equiv \Psi_1^*$ versus reduced shear rate. The right-hand side graph shows the α -dependence of the (reduced) shear rate a^* for the above three systems.

to every value of a^* is associated a given inelasticity, so that a^* vanishes in the elastic limit $\alpha \rightarrow 1$. This explains why the stationary temperature ratio converges to 1 in the small shear rate limit. For a given set of parameters m_1/m_2 , σ_1/σ_2 , and mole fraction x_1 , the curves displayed are obtained by scanning all possible inelasticity parameters α from 1 corresponding to a vanishing stationary shear rate, to $\alpha = 0$, which yields the maximum possible value of a^* (e.g. 0.24 for $x = 0.1$ for the parameters used in Fig. 7, as can be seen in both left and right hand side graphs). The equimolar case results have already been shown as the continuous curves in Figs. 1 and 3. Interestingly, it can be seen that the normal stress difference can become an increasing function of a^* (see the inset of Fig. 7), whereas it is decreasing within Model A, when α is fixed and a^* is changed. This is an illustration of the conflicting effects at work at the stationary point, when simultaneously increasing a^* and dissipation (indeed, Ψ_1^* decreases when α is fixed and a^* increases while it increases when a^* is fixed and α decreases). As far as the shear viscosity is concerned, the effects at work always lead to a decreasing function of a^* , as with fixed dissipation within Model A.

5. Conclusions

We have determined the rheological properties (shear stress and normal stress difference) for a binary granular mixture in a uniform shear flow. The problem has been addressed in the framework of the Boltzmann equation with Maxwell kernel. An important advantage of such a model – compared to the more realistic inelastic hard sphere kernel – is that the collisional moments can be obtained exactly, and do not require the explicit knowledge of the velocity distribution function of both species (only low order moments are required). It is important here to stress that in spite of its approximate nature, IMM have been shown to fare very favorably against Monte Carlo simulations of inelastic hard sphere mixtures [5,22]. We therefore expect the trends reported here to be realistic and of practical interest.

In the case of IMM, there is a characteristic frequency ν_0 that can be chosen freely. To study the rheological properties, two classes of models have been introduced. In Model A, ν_0 is taken independent from the total kinetic temperature T , while in Model B, ν_0 scales like T^q , with $q = 1/2$ to reproduce the hard-sphere behaviour. In this respect, Model A fundamentally differs from models with $q \neq 0$ in that it allows to disentangle the effects of dissipation (embodied in the coefficients of restitution α_{rs}) from those of imposed shear (embodied in the reduced shear rate a^* defined from the actual shear rate a by $a^* = a/\nu_0$). Indeed, whenever $q \neq 0$, the system reaches at long times a steady state where viscous heating

compensates for collisional cooling. In this steady state, a key point is that the reduced shear rate is enslaved to the inelasticity, so that the problem is inherently non-Newtonian [10] (in other words, it is not possible to decrease the reduced shear rate a^* by decreasing a , since then collisional dissipation will be more efficient and lead to a smaller granular temperature, so that a^* is finally unaffected). On the other hand, within Model A, inelastic dissipation and viscous heating *generically* do not compensate, so that the temperature of the system either grows without bounds, or decreases to 0. If, however, the reduced shear rate is adjusted to the precise value that is reached within Model B for a given parameter set, Model A admits a steady state (which is then identical to its Model B counterpart).

Outside the particular steady state point and within Model A, the scaled pressure tensor reaches well-defined stationary values which are non-linear functions of a^* and the coefficients of restitution α_{rs} . This allows for a clear-cut definition of the (reduced) non-linear shear viscosity η^* and normal stress difference Ψ_1^* (within Maxwell models, only one stress difference is non-vanishing, whereas there are two such quantities for the hard sphere kernel). These quantities have been computed for various parameters characterizing the mixture, and it has been found that when a^* is large enough (say $a^* > 1$), η^* and Ψ_1^* are insensitive to dissipation, mixture composition, mass ratio, and size ratio, but only depend on the shear rate. Both quantities decrease when a^* increases. At smaller shear amplitudes, the detailed parameters of the mixture becomes relevant and in particular we have found – for physically relevant dissipation parameters – that the shear viscosity and normal stress difference increase when dissipation is increased. The dependence on mixture composition and mass ratio appear more subtle, and are non-monotonous. Of particular interest also is the temperature ratio, which has been seen to depend on the parameters of the problem in a complex fashion.

Future developments include the study of the tracer limit, segregation of an intruder by thermal diffusion, together with a more general derivation of generalized transport coefficients from a Chapman–Enskog-like expansion [25]. Work along these lines is in progress.

Acknowledgments

This work was initiated during a visit of V.G. to the Laboratoire de Physique Théorique et Modèles Statistiques, Université Paris-Sud. He is grateful to this institution for its hospitality and support. The research of V.G. has been supported by the Ministerio de Educación y Ciencia (Spain) through grant No. FIS2007-60977, partially financed by FEDER funds and by the Junta de Extremadura (Spain) through Grant No. GRU08069.

Appendix A. Partial pressure tensors

The expression of the relevant elements of the partial pressure tensor P_i^* are given by

$$P_{1,xx}^* = \frac{1}{\Delta^3} \left\{ G\Delta^2 B_{12}^* + 2a^{*2} G B_{12} \left[3\lambda^2 + B_{11}^* + B_{12}^* B_{21}^* + B_{22}^* (B_{22}^* + 3\lambda) + B_{11}^* (B_{22}^* + 3\lambda) \right] - F\Delta^2 (B_{22}^* + \lambda) - 2a^{*2} F \left[B_{11}^* B_{12}^* B_{21}^* + B_{12}^* B_{21}^* (2B_{22}^* + 3\lambda) + (B_{22}^* + \lambda)^3 \right] \right\}, \quad (\text{A.1})$$

$$P_{1,yy}^* = \frac{G B_{12} - F(B_{22} + \lambda)}{\Delta}, \quad (\text{A.2})$$

$$P_{1,xy}^* = -\frac{a^*}{\Delta^2} \left\{ F \left[B_{12} B_{21} + (B_{22} + \lambda)^2 \right] - G B_{12} (B_{11} + B_{22} + 2\lambda) \right\}, \quad (\text{A.3})$$

where

$$\Delta = B_{12}^* B_{21}^* - (B_{11}^* + \lambda)(B_{22}^* + \lambda), \quad (\text{A.4})$$

$$F = A_{11}^* p_1^* + A_{12} p_2^*, \quad (\text{A.5})$$

$$G = A_{22}^* p_2^* + A_{21} p_1^*. \quad (\text{A.6})$$

In the above equations, $A_{rs}^* = A_{rs}/v_0$ and $B_{rs}^* = B_{rs}/v_0$ where A_{rs} and B_{rs} are given by Eqs. (27)–(30). The expressions for $P_{2,ij}^*$ can easily be obtained from (A.1)–(A.3) by the adequate changes of indices.

References

- [1] S. Chapman, T.G. Cowling, *The Mathematical Theory of Nonuniform Gases*, Cambridge University Press, Cambridge, 1970.
- [2] J.J. Brey, J.W. Dufty, C.S. Kim, A. Santos, Hydrodynamics for granular flow at low-density, *Phys. Rev. E* 58 (1998) 4638–4653; V. Garzó, J.M. Montanero, Transport coefficients of a heated granular gas, *Physica A* 313 (2002) 336–356.
- [3] See for instance, C.K.K. Lun, S.B. Savage, D.J. Jeffrey, N. Chepurini, Kinetic theories for granular flow: inelastic particles in Couette flow and slightly inelastic particles in a general flow field, *J. Fluid Mech.* 140 (1984) 223–256; J.T. Jenkins, M.W. Richman, Plane simple shear of smooth inelastic circular disks: the anisotropy of the second moment in the dilute and dense limits, *J. Fluid Mech.* 192 (1988) 313–328; N. Sela, I. Goldhirsch, S.H. Noskovicz, Kinetic theoretical study of a simple sheared two-dimensional granular gas to Burnett order, *Phys. Fluids* 8 (1996) 2337–2353; J.J. Brey, M.J. Ruiz-Montero, F. Moreno, Steady uniform shear flow in a low density granular gas, *Phys. Rev. E* 55 (1997) 2846–2856; J.M. Montanero, V. Garzó, A. Santos, J.J. Brey, Kinetic theory of simple granular shear flows of smooth hard spheres, *J. Fluid. Mech.* 389 (1999) 391–411; V. Garzó, Tracer diffusion in granular shear flows, *Phys. Rev. E* 66 (2002) 021308; J.F. Lutsko, Rheology of dense polydisperse granular fluids under shear, *Phys. Rev. E* 70 (2004) 061101.
- [4] See for instance, A.V. Bobylev, J.A. Carrillo, I.M. Gamba, On some properties of kinetic and hydrodynamic equations for inelastic interactions, *J. Stat. Phys.* 98 (2000) 743–773; J.A. Carrillo, C. Cercignani, I.M. Gamba, Steady states of a Boltzmann equation for driven granular media, *Phys. Rev. E* 61 (2000) 7700–7707; E. Ben-Naim, P.L. Krapivsky, Multiscaling in inelastic collisions, *Phys. Rev. E* 61 (2000) R5–R8; C. Cercignani, Shear flow of a granular material, *J. Stat. Phys.* 102 (2001) 1407–1415; M.H. Ernst, R. Brito, Scaling solutions of inelastic Boltzmann equations with over-populated high-energy tails, *J. Stat. Phys.* 109 (2002) 407–432; E. Ben-Naim, P.L. Krapivsky, The inelastic Maxwell model, *Granular Gas Dynamics*, in *Lecture Notes in Physics* 624 (2003) 65–94.
- [5] V. Garzó, Nonlinear transport in inelastic Maxwell mixtures under simple shear flow, *J. Stat. Phys.* 112 (2003) 657–683.
- [6] E. Trizac, P. Krapivsky, Correlations in ballistic processes, *Phys. Rev. Lett.* 91 (2003) 218302; F. Coppex, M. Droz, E. Trizac, Maxwell and very hard particle models for probabilistic ballistic annihilation: hydrodynamic description, *Phys. Rev. E* 72 (2005) 021105.
- [7] A. Santos, V. Garzó, Simple shear flow in inelastic Maxwell models, *J. Stat. Mech.* P08021 (2007).
- [8] K. Kohlstedt, A. Snezhko, M.V. Sapozhnikov, I.S. Arnarson, J.S. Olafsen, E. Ben-Naim, Velocity distributions of granular gases with drag and with long-range interactions, *Phys. Rev. Lett.* 95 (2005) 068001.
- [9] I. Goldhirsch, Rapid granular flows, *Annu. Rev. Fluid Mech.* 35 (2003) 267–293.
- [10] A. Santos, V. Garzó, J.W. Dufty, Inherent rheology of a granular fluid in uniform shear flow, *Phys. Rev. E* 69 (2004) 061303.
- [11] C. Truesdell, R.G. Muncaster, *Fundamentals of Maxwell's Kinetic Theory of a Simple Monatomic Gas*, Academic Press, New York, 1980.
- [12] V. Garzó, A. Santos, *Kinetic Theory of Gases in Shear Flows*. Nonlinear Transport, Kluwer Academic, Dordrecht, 2003.
- [13] M.H. Ernst, E. Trizac, A. Barrat, The rich behaviour of the Boltzmann equation for dissipative gases, *Europhys. Lett.* 76 (2006) 56–62; M.H. Ernst, E. Trizac, A. Barrat, The Boltzmann equation for driven systems of inelastic soft spheres, *J. Stat. Phys.* 124 (2006) 549–586; A. Barrat, E. Trizac, M.H. Ernst, Quasi-elastic solutions to the nonlinear Boltzmann equation for dissipative gases, *J. Phys. A: Math. Theor.* 40 (2007) 4057–4076.
- [14] See for instance, J.M. Montanero, V. Garzó, Monte Carlo simulation of the homogeneous cooling state for a granular mixture, *Granular Matter* 4 (2002) 17–24; A. Barrat, E. Trizac, Molecular dynamics simulations of vibrated granular gases, *Physical Review E* 66 (2002) 051303; A. Barrat, E. Trizac, Lack of energy equipartition in homogeneous heated binary granular mixtures, *Granular Matter* 4 (2002) 57–63; S.R. Dahl, C.M. Hrenya, V. Garzó, J.W. Dufty, Kinetic temperatures for a granular mixture, *Phys. Rev. E* 66 (2002) 041301; R. Pagnani, U.M.B. Marconi, A. Puglisi, Driven low density granular mixtures, *Phys. Rev. E* 66 (2002) 051304; P. Krouskop, J. Talbot, Mass and size effects in three-dimensional vibrofluidized granular mixtures, *Phys. Rev. E* 68 (2003) 021304; H. Wang, G. Jin, Y. Ma, Simulation study on kinetic temperatures of vibrated binary granular mixtures, *Phys. Rev. E* 68 (2003) 031301; J.J. Brey, M.J. Ruiz-Montero, F. Moreno, Energy partition and segregation for an intruder in a vibrated granular system under gravity, *Phys. Rev. Lett.* 95 (2005) 098001; M. Schröter, S. Ulrich, J. Krefl, J.B. Swift, H.L. Swinney, Mechanisms in the size segregation of a binary granular mixture, *Phys. Rev. E* 74 (2006) 011307.

- [15] R.D. Wildman, D.J. Parker, Coexistence of two granular temperatures in binary vibrofluidized beds, *Phys. Rev. Lett.* 88 (2002) 064301; K. Feitosa, N. Menon, Breakdown of energy equipartition in a 2D binary vibrated granular gas, *Phys. Rev. Lett.* 88 (2002) 198301.
- [16] V. Garzó, J.W. Dufty, Homogeneous cooling state for a granular mixture, *Phys. Rev. E* 60 (1999) 5706–5713.
- [17] A.W. Lees, S.F. Edwards, The computer study of transport processes under extreme conditions, *J. Phys. C* 5 (1972) 1921–1929.
- [18] M. Tij, E.E. Tahiri, J.M. Montanero, V. Garzó, A. Santos, J.W. Dufty, Nonlinear Couette flow in a low density granular gas, *J. Stat. Phys.* (2001) 1035–1068.
- [19] F. Vega Reyes, V. Garzó, A. Santos, Impurity in a granular gas under nonlinear Couette flow, *J. Stat. Mech.* P09003 (2008).
- [20] V. Garzó, A. Santos, Third and fourth degree collisional moments for inelastic Maxwell models, *J. Phys. A: Math. Theor.* 40 (2007) 14927–14943.
- [21] V. Garzó, A. Astillero, Transport coefficients for inelastic Maxwell mixtures, *J. Stat. Phys.* 118 (2005) 935–971.
- [22] J.M. Montanero, V. Garzó, Rheological properties IN a low-density granular mixture, *Physica A* 310 (2002) 17–38.
- [23] C. Marín, V. Garzó, A. Santos, Transport properties in a binary mixture under shear flow, *Phys. Rev. E* 52 (1995) 3812–3820.
- [24] For mechanically equivalent particles, an explicit comparison with the results reported in [7] requires a mapping of time scales by a factor $(d+2)/2$. Indeed, the reduced shear rate a^* used here is related to the same quantity appearing in [7], which we denote a_{SG}^* , through $a^* = 2a_{SG}^*/(d+2)$. The rheological functions are likewise affected: denoting again with subscript SG the reduced shear viscosity and viscometric function derived in [7], we have $\eta^* = \frac{d+2}{2} \eta_{SG}^*$ and $\Psi_1^* = \left(\frac{d+2}{2}\right)^2 \Psi_{1,SG}^*$.
- [25] V. Garzó, Transport coefficients for an inelastic gas around uniform shear flow: linear stability analysis, *Phys. Rev. E* 73 (2006) 021304; V. Garzó, Shear-rate dependent transport coefficients for inelastic Maxwell models, *J. Phys. A: Math. Theor.* 40 (2007) 10729–10757.